Processing of Macroporous Titania Thin Films: From Multiscale Functional Porosity to Nanocrystalline Macroporous TiO_2

M. Cecilia Fuertes and Galo J. A. A. Soler-Illia*

Unidad de Actividad Química, Centro Atómico Constituyentes, Comisión Nacional de Energía Atómica, Av. Gral Paz 1499 (B1650KNA) San Martín, Buenos Aires, Argentina

Received December 7, 2005. Revised Manuscript Received February 20, 2006

Titania thin films with hierarchical pore structure (macropores and nested mesopores) were obtained in one step by a combination of sol−gel synthesis with controlled phase separation. Poly(ethylene glycol) (M_w = 2000) induces a phase separation upon film formation, producing macropores with controllable diameters between 0.1 and 2 μm. The macroporous texture can be tuned by changing the synthesis conditions and the post-treatment. The inorganic walls present mesoporosity with an interpore separation of 3−4 nm. The porous TiO_2 wall surface can be modified by incorporating organic functions by post-grafting. An adequate post-synthesis treatment leads to nanocrystalline walls (anatase) without microcracks. The films thus produced can find potential applications as optical or photovoltaic materials, sensors, depollutants, and so forth.

Introduction

In the last 10 years, the synthesis of complex materials with spatial organization in multiple scales has experienced strong advances,[1,2] opening the very active field of "organized matter chemistry".[3] The use of templates (surfactants, polymers, microspheres) in combination with sol−gel chemistry has permitted the creation of organized porous materials, with nanoscopic to microscopic pore size.[4] The advantages of these materials are multiple: high surface areas (200−1200 m^2/g for mesoporous materials), calibrated pore sizes (2−50 nm for mesoscale, 50 nm−10 μm for macroscale), and controlled wall composition. The pore surfaces can be in turn modified with organic groups, leading to multifunctional materials, which are particularly interesting in advanced analytical applications.[5−9]

In the case of mesoporous materials, supramolecular templates, such as micelles or liquid crystals, are used. Controlling porosity in the upper limit of the mesoporous and macroporous scale is achieved by the use of larger colloidal templates, such as latex or silica nanometric beads and emulsion or foam templating,[10−12] or by the use of controlled phase separation in the presence of solvent mixtures and polymers.[13,14] A combination of different templates (polymers and surfactants) permits the synthesis of hierarchical superstructures that present order at multiple length scales.[15−19]

The processing of these complex porous materials as thin oxide films with controlled porosity is particularly interesting to develop applications in optics, electronics, catalysis, sensing, and separation.[1,20−22] The design of multiscale (i.e., meso−macroporous) oxides is a step toward the creation of

* To whom correspondence should be addresed. E-mail: gsoler@cnea.gov.ar. Phone: (5411) 6772 7032. Fax: (5411) 6772 7886.

(1) Soler-Illia, G. J. A. A.; Sanchez, C.; Lebeau, B.; Patarin, J. *Chem. Rev.* **2002**, *102*, 4093.
(2) Sanchez, C; Arribart, H.; Giraud-Guille, M. M. *Nat. Mater.* **2005**, *4*, 277.
(3) Mann, S.; Burkett, S. L.; Davis, S. A.; Fowler, C. E.; Mendelson, N. H.; Sims, S. D.; Walsh, D.; Whilton, N. T. *Chem. Mater.* **1997**, *9*, 2300.
(4) Antonietti, M.; Ozin, G. A. *Chem.—Eur. J.* **2004**, *10*, 28.
(5) See for example *J. Mater. Chem.* **2005**, *15*, 3541−3988 (Special Issue on Functional Hybrid Materials).
(6) Shi, J. L.; Hua, Z. L.; Zhang, L. X. *J. Mater. Chem.* **2004**, *14*, 795 and references therein. See also Sayari, A.; Hammoudi, S. *Chem. Mater.* **2001**, *13*, 3151. Asefa, T.; Yoshina-Ishii, C.; MacLachlan, M. J.; Ozin, G. A. *J. Mater. Chem.* **2000**, *10*, 1751.
(7) Soler-Illia, G. J. A. A.; Innocenzi, P. *Chem.—Eur. J.*, published online Jan 23, 2006 http://dx.doi.org/10.1002/chem.200500801.
(8) *Functional Hybrid Materials*; Gómez Romero, P., Sanchez, C., Eds.; Wiley: New York, 2004.
(9) (a) Liu, J.; Shin, Y.; Nie, Z.; Chang, J. H.; Wang, L.-Q.; Fryxell, G. E.; Samuels, W. D.; Exarhos, G. J. *J. Phys. Chem. A* **2000**, *104*, 8328. (b) Dufaud, V.; Davis, M. E. *J. Am. Chem. Soc.* **2003**, *125*, 9403.
(10) (a) Wijnhoven, J. E. G.; Vos, W. L. *Science* **1998**, *281*, 802. (b) Jiang, P.; Bertone, J. F.; Colvin, V. L. *Science* **2001**, *291*, 5503 and references therein.
(11) (a) Imhof, A.; Pine, D. J. *Nature* **1997**, *389*, 948. (b) Holland, B. T.; Blanford, C. F.; Stein, A. *Science* **1998**, *281*, 538.
(12) Tetréault, N.; Míguez, H.; Ozin, G. A. *Adv. Mater.* **2004**, *16*, 1471.
(13) Nakanishi, K. *J. Porous Mater.* **1997**, *4*, 67.
(14) Bouchara, A.; Mosser, G.; Soler-Illia, G. J. A. A.; Chane-Ching, J.-Y.; Sanchez, C. *J. Mater. Chem.* **2004**, *14*, 2347.
(15) Yang, P.; Deng, T.; Zhao, D.; Feng, P.; Pine, D.; Chmelka, B. F.; Whitesides, G. M.; Stucky, G. D. *Science* **1998**, *282*, 2244.
(16) Sato, Y.; Nakanishi, K.; Hirao, K.; Jinnai, H.; Shibayama, M.; Melnichenko, Y. B.; Wignall, G. D. *Colloids Surf., A* **2001**, *187−188*, 117.
(17) Nakanishi, K.; Takahashi, R.; Nakagane, T.; Kitayama, K.; Koheiya, N.; Shikata, H.; Soga, N. *J. Sol.-Gel Sci. Technol.* **2000**, *17*, 191.
(18) (a) Nakanishi, K.; Kobayashi, Y.; Amatani, T.; Hirao, K.; Kodaira, T. *Chem. Mater.* **2004**, *16*, 3652. (b) Amatani, T.; Nakanishi, K.; Hirao, K.; Kodaira, T. *Chem. Mater.* **2005**, *17*, 2114.
(19) (a) Blin, J.-L.; Léonard, A.; Yuan, Z. Y.; Gigot, L.; Vantomme, A.; Cheetham, A. K.; Su, B. L. *Angew. Chem., Int. Ed.* **2003**, *42*, 2872. (b) Yuan, Z. Y.; Ren, T.-Z.; Vantomme, A.; Su, B. L. *Chem. Mater.* **2004**, *16*, 5096.
(20) (a) Nicole, L.; Boissière, C.; Grosso, D.; Quach, A.; Sanchez, C. *J. Mater. Chem.* **2005**, *15*, 3598. (b) Grosso, D.; Cagnol, F.; Soler-Illia, G. J. A. A.; Crepaldi, E. L.; Amenitsch, H.; Brunet-Bruneau, A.; Bourgeois, A.; Sanchez, C. *Adv. Funct. Mater.* **2004**, *14*, 309.
(21) Sanchez, C.; Soler-Illia, G. J. A. A.; Ribot, F.; Mayer, C.; Cabuil, V.; Lalot, T. *Chem. Mater.* **2001**, *13*, 3061.
(22) Otal, E. H.; Angelomé, P. C.; Bilmes, S. A.; Soler-Illia, G. J. A. A. *Adv. Mater.*, accepted (http://dx.doi.org/10.1002/adma.200502215).

10.1021/cm0527064 CCC: $33.50
Published on Web 03/16/2006

devices with porosity in the macroscale, which can enhance molecule transport or interact with large size biological species as bacteria or cells.

The combination of sol−gel processing with controlled phase separation, induced by polymers such as poly(ethylene glycol) (PEG)[13] or polypeptides,[14,23] is a simple strategy to produce macroporous oxide films. Titania macroporous thin films with enhanced surface area were produced aiming at improving their photocatalytic properties.[24] Nakanishi and co-workers made a pioneering exploration of the effect of the synthesis conditions in the film morphology,[25] and a comprehensive study of each variable was performed by Kajihara and Yao.[26−31] From this earlier work, it has been proposed that the PEG templating agent forms a stable complex with Ti−oxo species and that the macropores are generated by the phase separation of solvent. Authors make an analogy between the titania systems and previously explored silica macroporous gels. In principle, macroscopic domains are developed if solidification of the inorganic polymeric phase is produced after the phase separation which originates the pores. The phase separation process is induced by the strong interactions between the inorganic oligomers and the organic polymer, which repel the solvent. This results in micronic solvent droplets, which are the actual pore templates. If solidification is produced before phase separation, films withno apparent macropores are obtained. Film fluidity is required during the drying process to favor rearrangement of the nanobuilding units (in this case, Ti−oxo clusters) for the macropore formation. It is also important to avoid rapid drying to permit mobility of the oligomers, favor higher condensation grades, and avoid flaws formation. This "race towards size-controlled pores" is similar to what is found in mesoporous thin films produced by evaporation-induced self-assembly.[7,32]

Despite the insight gained in the synthesis conditions of titania macroporous films, two aspects still have to be clarified. First, even if the effect of the synthesis variables upon the macropore formation is beginning to be understood, the detailed texture of the inorganic walls upon synthesis is not known. This aspect is relevant, in view of the possibility of the formation of mesopores due to the processing conditions used (low water, high acidity, presence of a hydrophilic polymer).[33−35] The presence of mesopores implies the one-pot formation of thin films with hierarchical porosity. Second, scarce information about the effects of film processing (i.e., post-synthesis conditioning and dependence on the thermal treatment) in the final film features (porosity, absence of cracks, pore definition, nature of the wall nanocrystalline structure, etc.) is available. This aspect is crucial for applications where particular wall texture and film quality are desired.

Table 1. Compositions of the Solutions Used in This Work (Molar Composition)

solution	TET	PEG 2000	ethanol	butanol	H_2O	HNO_3
A	1		8.33		0.83	0.167
P1	1	0.02	8.33		0.83	0.167
P2	1	0.02	4.17	2.58	0.83	0.167

In this work, we focused the efforts in the two aspects cited above. Titania macroporous films were synthesized by dip-coating, from alcohol−water solutions containing Ti(IV) precursors and PEG with $M_w = 2000$ (PEG 2000), at a given Ti(IV) concentration, and fixed ratios $h = [H_2O]/[Ti] = 0.83$ and $p = [H^+]/[Ti] = 0.17$, a composition close to those previously explored.[25,26,29] Several external synthesis variables such as relative humidity (RH%) during synthesis and processing, withdrawal speed (S_w), or sol temperature (T) were systematically changed, to obtain a variety of textures: nonmacroporous, macroporous, or cracked. The systematic observation of the parameter texture space led to the construction of "processing windows", where the global effect of these important synthesis variables in the film texture was observed. These processing windows permit the adequate conditions for the development of macropores upon solvent evaporation at 25 °C < T < 50 °C to be defined, which was confirmed by crossed scanning electron microscopy (SEM) and Fourier transform infrared (FTIR) observations. Transmission electron microscopy (TEM) observation revealed that the titania walls of films calcined up to 300 °C are mesoporous. Thus, organic functions can be added to the pore surface, leading to functional films with hierarchical macro/mesoporous texture. In addition, an adequate postprocessing of the macro-mesoporous titania films permits the production of crack-free crystalline thin films (anatase) with tailored vertical macropores.

Experimental Section

Titanium tetraethoxide (TET: $Ti(OC_2H_5)_4$, Fluka, 98%) was used as received. PEG 2000 (hereafter, PEG) was used as a texture-directing agent. Starting solutions were prepared as follows. First, TET was dissolved in half of the prescribed amount of ethanol (or the ethanol−butanol mixture). The other half was mixed with water and nitric acid (to hinder Ti(IV) condensation); this mixture was added dropwise to the solution containing Ti(IV) under ice-cooled conditions with vigorous stirring. A prescribed amount of PEG was subsequently added to the resulting solution, and the container was sealed and placed in water at 40 °C for 30 min under stirring for PEG dissolution. Final compositions of the solutions named A, P1, and P2 (mole ratio) are listed in Table 1. Nonmacroporous films were produced using precursor mixture A in the absence of PEG, for control experiments. These dense films were submitted to the same treatment as the PEG-containing films and were used as a reference for the refraction index of the titania walls.

Titania films were produced by dip-coating, at a variable withdrawal speed (S_w) between 0.1 and 2 mm/s. Clean glass, silicon wafers, or KBr pellets were used as substrates. Synthesis parameters

(23) Bouchara, A.; Soler-Illia, G. J. A. A.; Chane-Ching, J.-Y-; Sanchez, C. *Chem. Commun.* **2002**, 1234.
(24) Kato, K.; Tsuzuki, A.; Torii, Y.; Taoda, H.; Kato, T.; Butsugan, Y. *J. Mater. Sci.* **1995**, *30*, 837.
(25) Kajihara, K.; Nakanishi, K.; Tanaka, K.; Hirao, K.; Soga, N. *J. Am. Ceram. Soc.* **1998**, *81*, 2670.
(26) Kajihara, K.; Yao, T. *J. Sol.-Gel Sci. Technol.* **1998**, *12*, 185.
(27) Kajihara, K.; Yao, T. *J. Sol.-Gel Sci. Technol.* **1998**, *12*, 193.
(28) Kajihara, K.; Yao, T. *J. Sol.-Gel Sci. Technol.* **1999**, *16*, 257.
(29) Kajihara, K.; Yao, T. *J. Sol.-Gel Sci. Technol.* **2000**, *17*, 173.
(30) Kajihara, K.; Yao, T. *J. Sol.-Gel Sci. Technol.* **2000**, *17*, 239.
(31) Kajihara, K.; Yao, T. *J. Sol.-Gel Sci. Technol.* **2000**, *19*, 219.
(32) Brinker, C. J.; Lu, Y.; Sellinger, A.; Fan, H. *Adv. Mater.* **1999**, *11*, 579.
(33) Blanchard, J.; Ribot, F.; Sanchez, C.; Bellot, P.-V.; Trokiner, A. *J. Non-Cryst. Solids* **2000**, *265*, 83.
(34) Soler-Illia, G. J. A. A.; Sanchez, C. *New J. Chem.* **2000**, *24*, 493.
(35) Soler-Illia, G. J. A. A.; Scolan, E.; Louis, A.; Albouy, P.-A.; Sanchez, C. *New J. Chem.* **2001**, *25*, 154.

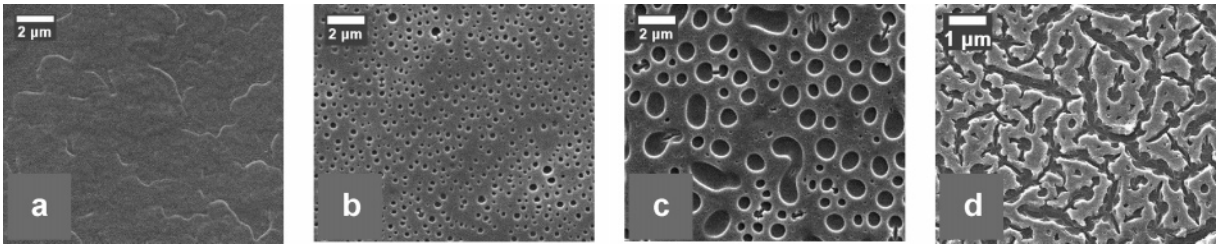

Figure 1. SEM micrographs of titania films obtained from the same starting solution (P1) under different synthesis conditions: (a) $S_w = 2$ mm/s, $T = 30$ °C, and RH% = 50%; (b) $S_w = 0.2$ mm/s, $T = 35$ °C, and RH% = 50%; (c) $S_w = 0.5$ mm/s, $T = 30$ °C, and RH% = 50%; and (d) $S_w = 0.2$ mm/s, $T = 40$ °C, and RH% = 50%. All films were subsequently treated at 250 °C.

(solution temperature, withdrawal speed, humidity inside the dip-coating chamber, and post-treatment) have to be precisely controlled to obtain a well-defined macroporous texture. In particular, control of the RH upon film deposition is essential, as has been proven in the case of mesoporous thin films.[36,37] The dipping operation was performed at a given sol temperature between 20 and 50 °C. As-prepared films were submitted to consecutive 24-h treatments at 50% RH, 60 °C, and 130 °C to improve cross-linking of the inorganic network and favor microphase separation.[37] Thermal treatment of these stabilized coatings was performed in tubular ovens, under still air, using 1 °C min^{-1} temperature ramps, up to 250 °C, and maintained for 2 h, to eliminate the PEG. Thermal treatments at higher temperatures (400−500 °C) were performed to crystallize the walls.

The accessibility of the pore systems was studied by following the adsorption of organic molecules, which can form intensely colored complexes with Ti centers (such as 1,2-dihydroxybenzene-3,5-sodium disulfonate, hereafter TIRON) or which bear long aliphatic chains (dihexadecyl phosphate, hereafter DHDP), and can be detected by FTIR, as previously reported for titania mesoporous thin films.[38] A typical functionalization experiment was performed by dipping a calcined film in a continuously stirred solution of the chosen molecule. The immersion time (t_{uptake}) was varied from 5 min to several hours.

Film texture in the macroscale and thickness were studied by SEM (Philips 515 equipped with EDS). TEM (Philips CM 200) was used to observe the composition and the texture in the mesoscale and to assess the crystalline nature of the matrix by selected-area electron diffraction (SAED). Thermal analysis (differential thermal analysis−thermogravimetric analysis, DTA-TGA) was performed with a Shimadzu DTG-50 (1 °C min^{-1}) in air. X-ray diffraction (XRD) patterns were collected in θ-2θ mode using a conventional goniometer PW 1820 Philips (Cu Kα_1 radiation). Several macroporous films were scratched to obtain powder (16.7 mg) for N_2 adsorption measurements (Micromeritics ASAP 2010). Organic molecule adsorption was followed by UV−visible spectroscopy (Hewlett-Packard 8453) and infrared spectroscopy (FTIR, Nicolet Magna 560). The elimination of the structuring agent was studied by FTIR of films thermally treated at a given temperature for a given period. Finally, transparent nonporous or mesoporous films deposited on silicon were analyzed by ellipsometry (Sentech SE 400), to assess thickness, refraction index, and porosity; the latter was evaluated by considering air-filled pores in a titania matrix and a simple Maxwell−Garnett approximation.[39]

Results and Discussion

(1) Synthesis of Macroporous Films. When the synthesis strategy reported in the literature and sketched above is used, the porosity in the micrometer scale can be tuned by changing the solution composition, processing, and post-processing of the films. Figure 1 shows typical SEM micrographs of macroporous titania films synthesized in different conditions, subsequently heated to 250 °C.[40] These micrographs depict the variety of textures that can be obtained from a solution with P1 composition, by changing the synthesis and post-treatment conditions. Transparent films without macropores are shown in Figure 1a; films presenting different pore diameters are shown in Figure 1b (0.1 μm) or Figure 1c (1 μm). In some conditions, films develop macroscopic cracks (Figure 1d).

To produce macroporous films in a reproducible way, it is necessary to accurately control the three most important synthesis parameters, apart from solution composition: (a) withdrawal speed, S_w, (b) solution temperature, and (c) %RH inside the dip-coating chamber. The final textures obtained in this complex system derive from the strong interdependence of these three variables, which in turn govern (i) the solvent evaporation rate, (ii) the emergence of phase separation, and (iii) the changes in the film viscosity. These three factors determine the features of the final film texture.

By performing a systematic exploration using solutions P1 and P2, two processing windows can be found that lead to obtaining macroporous crack-free films. The thickness of the as-deposited film, which is mainly determined by the withdrawal speed, is one of the most critical parameters. Therefore, we studied the relationship between withdrawal speed and solution temperature, at a constant RH (Figure 2a), and the correlation between the withdrawal speed with the RH, at constant solution temperature (Figure 2b).

Figure 2a shows the dependence of the textures obtained at different temperatures at a given S_w, for a constant %RH = 50%. The observed trends are coincident with those obtained in previous work,[31] where a more reactive titanium precursor is used. In both cases, the stability domain of the well-defined macroporous texture forms a diagonal, indicating that both synthesis parameters have crossed effects in the film formation, which lead to an optimum S_w value for each temperature. At temperatures between 25 and 35 °C, well-defined macropores (M) develop at low S_w values.

(36) Cagnol, F.; Grosso, D.; Soler-Illia, G. J. A. A.; Crepaldi, E. L.; Babonneau, F.; Amenitsch, H.; Sanchez, C. *J. Mater. Chem.* **2003**, *13*, 61.
(37) Crepaldi, E. L.; Soler-Illia, G. J. A. A.; Grosso, D.; Cagnol, F.; Ribot, F.; Sanchez, C. *J. Am. Chem. Soc.* **2003**, *125*, 9770.
(38) (a) Angelomé, P. C.; Aldabe-Bilmes, S.; Calvo, M. E.; Crepaldi, E. L.; Grosso, D.; Sanchez, C.; Soler-Illia, G. J. A. A. *New J. Chem.* **2005**, *29*, 59. (b) Angelomé, P. C.; Soler-Illia, G. J. A. A. *Chem. Mater.* **2005**, 17, 322.
(39) Maxwell-Garnett, J. C. *Philos. Trans. R. Soc. London* **1906**, *203*, 385.
(40) Unless stated otherwise, SEM micrographs presented in this work correspond to titania films thermally treated at 250 °C.

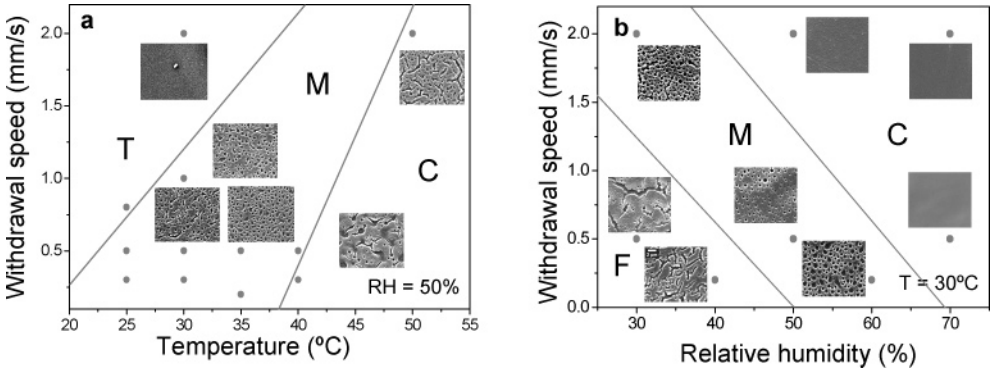

Figure 2. Processing windows for (a) P1 and (b) P2 systems. M, macropores; T, transparent film; C, film with cracks.

Nonmacroporous transparent (T) films are obtained at higher S_w. For example, for $S_w > 1$ mm/s at 30 °C, thicker films are formed and polycondensation of Ti(IV) can take place, as a result of the longer drying times. This leads to more viscous films, hindering phase separation.[31] At higher temperature, solvent evaporation and polycondensation are spurred. For low S_w values, both processes occur rapidly, generating tensions, and, therefore, cracked films (C) with or without macropores are obtained. Slightly higher speeds are needed to attain an optimum thickness for macropore development at $T > 40$ °C.

Figure 2b depicts the texturing effects in the S_w versus RH% field, for a system using an ethanol/butanol solvent mixture. Again, a "diagonal" trend is observed, which is in good agreement to the one observed in previous work using ethanolic solutions.[26] The thinnest films (i.e., lowest S_w)[41] produced at lower RH% values present the same tension problems commented on above, originating in rapid solvent evaporation, and thus develop cracks. On the other extreme, solvent evaporation in thicker films is slower. This effect, combined with high humidity, enhances both the condensation rate and the PEG solubility, thus hindering phase separation. Therefore, the optimum conditions to obtain a well-defined macropore lie in an intermediate region. Macroporous domains are formed at a moderate withdrawal speed, when films are relatively thinner. In these conditions, the phase separation occurs before gelation takes place, during the deposition and post-treatment.

The correlations observed in Figure 2 are coincident with those reported in earlier work,[24−31] while covering a more extended value range for each parameter and permitting a larger view of the general trends of macropore formation. The presentation in the form of processing window diagrams provides a useful tool to design the synthesis route and permits a better understanding of the forces driving the pore formation.

A distinctive feature of this kind of system is that several relevant system variables such as temperature or humidity have crossed effects on the *evaporation*, *stiffening of the deposited gel phase*, and *phase separation* processes. Thus, a complete analysis of the pore formation in these systems is complex. The general trends can be understood by taking into account the competition of processes favoring the phase separation, such as solvent evaporation rate, polymer insolubility in alcohol, and critical concentrations for phase separation, versus the processes hindering phase separation: inorganic condensation and increase of the viscosity. In addition, the temperature and RH dependence of all these processes are different, and this can affect the pore formation upon solvent evaporation in opposite ways. For example, higher temperatures lead to a faster solvent evaporation and faster inorganic condensation, as discussed above. At higher temperatures, polymer solubility in the bulk solvent is higher, retarding the phase separation. However, viscosity is reduced, permitting an easier matter transport and, thus, favoring phase separation. The actual behavior of the system will derive from the relative dependences of all these opposed processes with the temperature or RH change. To discuss in a complete fashion the formation mechanism, all these aspects have to be taken into account. Further research is being performed about this subject.

(2) Thermal Treatment: Macropore Formation and Template Elimination. To design reproducible synthesis methods, it is essential to understand the mechanism of macropore formation. In the particular case of thin films, the processing windows are narrow due to the great influence of the environment during dip-coating and the subsequent processing, as has been well-documented in mesostructured thin films.[7,20b,36,37] A variety of synthesis and post-processing conditions were studied, and it has been found that the effect of the variables (solution temperature, humidity, fwithdrawal speed, etc.) is complex and that the post-synthesis treatment is fundamental to consolidate the pore structure.[42] In addition, the existing information about the intermediate stages in the formation of pores, from the solution to the ceramic film, is scarce.

Immediately after the deposition by dip-coating, hybrid organic−inorganic films containing a Ti−oxo framework and PEG are obtained. DTA-TGA experiments were carried out to determine the processes taking place upon thermal treatment. Figure 3 presents a typical DTA-TGA run, under air flow. Three weight losses are observed: (a) below 100 °C (10%), (b) 120−160 °C (8%), and (c) 220−270 °C (20%); steps b and c are coincident with exothermic DTA peaks. These weight losses can be attributed to the loss of solvent,

(41) Brinker, C. J.; Scherer, G. W. *Sol-Gel Science*; Academic Press: New York, 1990.

(42) Fuertes, M. C. Films delgados macro y mesoporosos: arquitecturas supramoleculares para el diseño de materiales avanzados. M.Sc. Thesis, Universidad Nacional de San Martín, San Martín, 2005 (IT/T 94/05, available upon request).

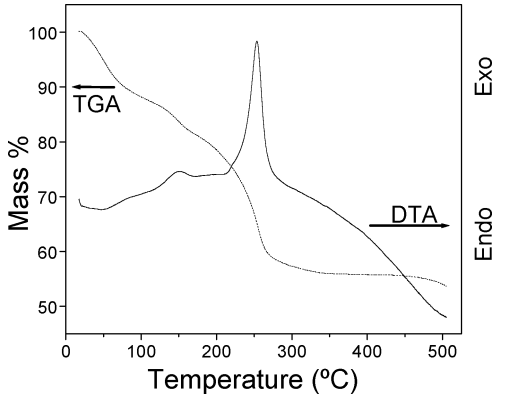

Figure 3. Thermal analysis of a solid xerogel obtained from the P1 system, in an air atmosphere.

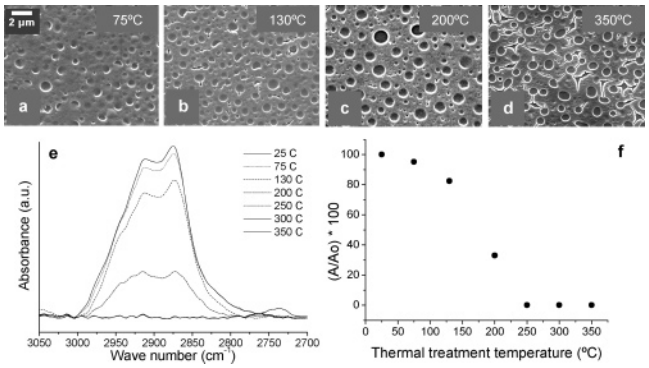

Figure 4. (a−d) SEM micrographs of films at different temperatures (all micrographs are in the same scale). (e, f) Evolution of the ν_{CH} band of PEG with temperature, measured by FTIR.

liberation of pending alcoxy groups, and PEG elimination, respectively. The thermal evolution features are similar to those observed in titania mesoporous materials synthesized in similar conditions (i.e., titanium alkoxides or ionic or nonionic organic templates).[43]

Hybrid films and xerogels (i.e., containing PEG) were studied by crossing FTIR and SEM to evaluate the macroporosity evolution along synthesis and post-treatment. Experiments were performed by submitting freshly prepared samples at increasing temperature during successive 30 min periods (i.e., variable temperature experiments) or by submitting samples previously stabilized at 130 °C to a constant temperature of 200 °C for variable time intervals (i.e., variable time experiments).

FTIR and SEM information of films synthesized from P1 solutions (S_w = 0.375 mm/s, 40 °C, and 50% RH) and submitted to variable temperature (from 25 to 350 °C) during 30 min intervals is presented in Figure 4. Immediately after the dip-coating operation, films produced in these conditions are opaque. Thus, phase separation in the micrometer scale occurs at ambient temperature, before thermal treatment. SEM micrographs of samples treated at 75 °C depict a surface with incipient pores (Figure 4a); these macrodomains become increasingly defined at intermediate temperatures (Figure 4b), and turn to well-defined pores at 200 °C (Figure 4c). These morphological and textural changes occur together with the decrease of the FTIR band area between 2800 and 3000 cm^{-1} (ν_{CH} vibrations) with increasing temperature. These bands correspond to the ethylene groups of PEG and the remaining methylene and ethylene groups corresponding

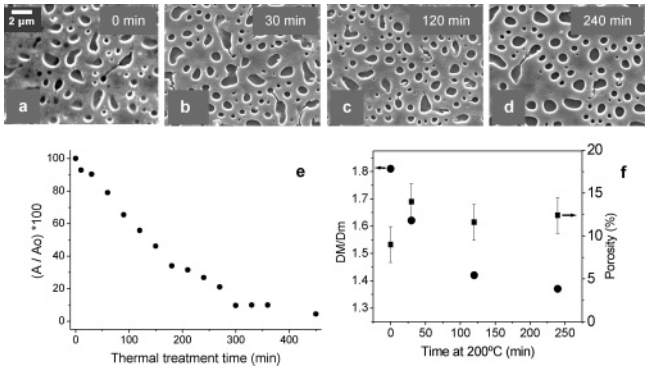

Figure 5. (a−d) SEM micrographs of films at 200 °C for different times (all micrographs are in the same scale); (e) decreases of the ν_{CH} band of PEG with time at 200 °C, measured by FTIR; and (f) evolution of the porosity and change in the pore morphology with time.

to weakly attached alcohol and alkoxy groups. Figure 4e,f shows the evolution of the relative ν_{CH} band area ($A(T)/A_0$, where A_0 is the initial band area for the as-synthesized film and $A(T)$ is the band area at a given temperature, T). Two stages are observed:

(1) Before 150 °C, the band area decrease is small, corresponding to residual ethanol elimination and/or decomposition of the dangling Ti−OEt groups, the consequence of an incomplete condensation (as seen by TGA). This stage is coincident with a progressively better definition of the macropores, as seen by SEM.

(2) After 200 °C, the disappearance of the FTIR ν_{CH} absorption is more evident. This is coincident with the DTA-TGA results. From these results, it can be concluded that the PEG is eliminated in this stage. SEM images show a perfectly developed macropore system, with well-defined pores. The macropore structure is retained at 350 °C, where some cracks begin to appear in these processing conditions.

From the variable temperature experiments, it can be concluded that the macropores are formed in the first stages after dip-coating and that a significant fraction of PEG is present in the film at 200 °C, when the pores are well-defined.

Variable time experiments are useful to follow the processes taking place within the film upon heating. At 200 °C, all solvent and pending −OR groups have been eliminated, and PEG begins to decompose; however, no massive PEG decomposition is observed. SEM images (Figure 5a−d) and FTIR spectra were obtained every 30 min for 7 h. A gradual loss of the ν_{CH} vibrations is observed; as a result of the loss of ethoxy and PEG fragments, 50% of the organic is eliminated before 2 h of treatment, and 90% is removed within 5 h (Figure 5e). SEM micrographs show initially well-defined albeit asymmetric pores present at low temperature in the stabilized hybrid films. This pore morphology could be related with a transient structure formed by spinodal decomposition. The total macropore surface (estimated as the visible substrate area by image analysis) changes by a small amount, within experimental error (Figure 5f), within the first 120 min; this fact is in agreement with the minor pore size increase along thermal treatment previously found.[29] The pores also tend to round off along the first 100−120 min of aging (Figure 5f). These three independent results demonstrate that several compositional and macrostructure

rearrangements occur within the first 120 min at 200 °C. After that period, major textural changes (for example, the rounding of the pores) are slower or even halted. This suggests that the initial inorganic skeleton presents a given flexibility, which can be associated with the presence of PEG.

As discussed above, the macropore structure is well-developed in films stabilized at 130 °C, and most C−H vibrations should correspond to the PEG backbone. Major changes in the pore morphology occur while a significant amount of PEG is present in the film. While these changes do not seem to modify appreciably the substrate surface covered by the film (i.e., the "pore area"), the pores tend to attain a rounded shape. This minimizes the perimeter/area ratio of the pores, therefore minimizing the surface area of the oxide film. Thus, a simple surface energy minimization should be the driving force for the pore shape evolution. Despite this process being thermodynamically favored, kinetics plays a central role, and the necessary rearrangements occur preferentially in the presence of an important fraction of the polymer, which facilitates the rearrangements of the oxide skeleton.

The presence of PEG intimately "entangled" with the inorganic network imparts flexibility to the film framework, either by separating the Ti−oxo building blocks (thus, preventing extended condensation) or by changing the mechanical properties of the composite, thus permitting a higher film fluidity. When an important fraction of the PEG is eliminated (Figure 5e), the processes leading to textural change are hindered; evolution toward the most stable texture is halted. Therefore, we can indirectly conclude that at least a fraction of the PEG is associated with the Ti−oxo network, as proposed by Kajihara et al.[25] The flexibility of the organic−inorganic network is coherent with what has been observed in Ti−oxo networks in the presence of nonionic[34,35] or cationic[43] surfactants, and requires the following:

(i) A sol−gel system where the Ti−oxo condensation is not fully extended. It is well-known that in the sol−gel conditions explored in this work, the sub-stoichiometric water quantities (added in the initial solution or incoming from the environment) generate small cluster-like Ti−oxo species.[33]

(ii) A close association of these cluster-like species with the ethylene oxide ($-CH_2-CH_2-O-$) fragments of the PEG chains, either by H-bonding or by complexation of the Ti(IV) centers by the (poly)ether moieties.[34]

In conclusion, while PEG is present in the initial hybrid macroporous film and the Ti−oxo species are not fully interconnected, the PEG/Ti−oxo system is flexible. The thermal treatment eliminates the PEG and helps to complete the condensation of the inorganic network, stiffening the framework. A careful post-synthesis treatment, with a well-designed sequence of post-treatment stabilization steps and a moderate thermal treatment, can assist the evolution of the initially formed films to a morphology of round-shaped pores, which is the most stable.

(3) Mesoporous Walls. The experiments discussed above indicate that the PEG is associated to the Ti−oxo clusters, which form the wall backbone. An interesting additional aspect is the possibility of further PEG microphase separation from the Ti−oxo framework, which can lead to a mesoporous texture. The existence of a secondary texture has not been so far reported in PEG−titania macroporous films.

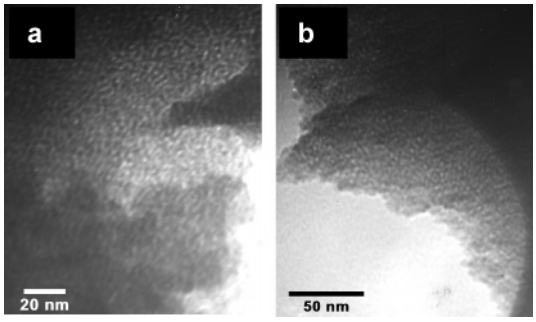

Figure 6. TEM micrographs of the system P1, showing the mesostructured walls for two different synthesis conditions: (a) transparent film (T) and (b) macroporous film (M).

To determine if the PEG generates an additional texture in the mesoscale, films with and without macropores were prepared from solution P1 and analyzed by TEM. By changing the synthesis conditions, the film evolution can be "frozen" before macropore formation, as discussed above. Films without macropores (Figure 1a) are transparent (hereafter, T). Films with macropores (Figure 1b) are opaque (hereafter, M). In addition, dense titania films prepared using solution A without PEG (D films) were synthesized as a control experiment.[44]

Figure 6 shows TEM micrographs of T (Figure 6a) and M films (Figure 6b) calcined at a temperature of 250 °C for 120 min, conditions adequate enough to eliminate all organic components. In both cases, a "wormlike" pattern in the mesoscale can be observed throughout the samples, indicating the presence of a mesostructured porous system; this texture was absent in the control D films. Analysis of the TEM images with ImageJ software[45] permits the determination of the mesopore diameter (d) and the interpore distance (IPD), which were essentially the same for both kinds of porous films (T and M): $d \approx 2.0 \pm 0.3$ nm and IPD $\approx 4.0 \pm 0.3$ nm. Although no reliable mesopore diameter values could be obtained by N_2 adsorption isotherms, because of the limitations in the sample quantity, these macroporous films present a specific surface area of 60 m^2/g, as determined by BET analysis.

The film porosity can be independently evaluated by ellipsometry. D and T films were deposited on silicon and calcined for 2 h at 250 °C. The refraction index ($n = 2.072$) of the dense films (D) is a good estimation of the wall refraction index of porous thin films submitted to the same process conditions.[38b] For T films, $n = 1.878$, leading to an estimated porosity of 18%. This porosity does not include the microporosity due to the sol−gel process, as the control experiment is done upon a sol−gel titania film synthesized in the same conditions. Therefore, the obtained porosity can be attributed to the mesoporosity observed by TEM.

(43) Soler-Illia, G. J. A. A.; Louis, A.; Sanchez, C. *Chem. Mater.* **2002**, *14*, 750.

(44) T and D films have been produced at $S_w = 2$ mm/s, $T = 30$ °C, and 45% RH; M films have been prepared at $S_w = 2$ mm/s, $T = 50$ °C, and 45% RH.

(45) *ImageJ*. Available from http://rsb.info.nih.gov/ij/.

Scheme 1. Processes Taking Place along the Formation of a Macro/Mesoporous TiO_2 Thin Film

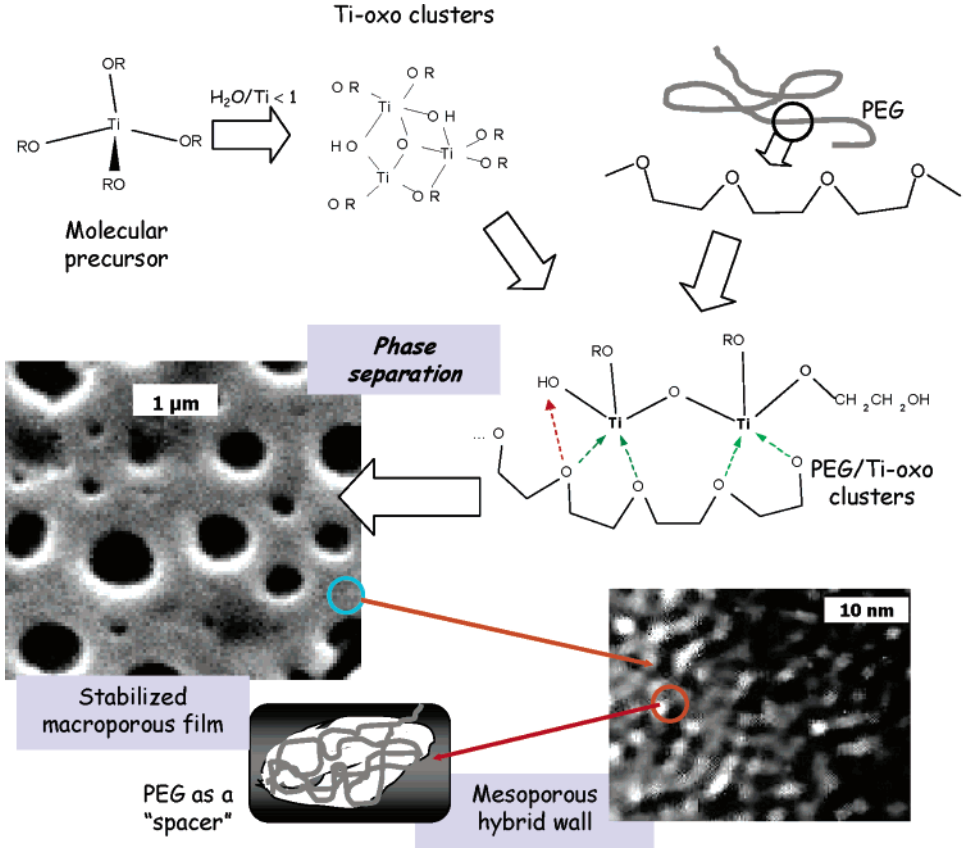

The TEM and porosity results indicate that, independently of the presence of macropores, a disordered mesoporous structure is obtained in T or M films. This mesostructure seems to be a consequence of a microphase separation between the PEG and the Ti−oxo network. These results are in excellent agreement to those found in Ti−oxo based mesoporous films and xerogels produced by combining Ti alkoxides and nonionic surfactant templates, in the presence of low water quantities.[34,35] In that case, mesopores are formed by the microphase segregation of polymer fragments, which are loosely attached to the Ti−oxo clusters. The nonionic surfactant does not form well-defined micellar entities, as the lack of water precludes differentiation between the hydrophilic and hydrophobic template regions. PEG acts merely as a polymeric spacer, leading to disordered pore systems. In the present work, a similar situation arises. Upon solvent evaporation, the interactions between PEG and the Ti−oxo clusters are essentially the same as in the preceding example; as a consequence, the observed mesoporosity has probably the same origin.

Therefore, the films present a nested pore network, composed of both macropores and mesopores. A macroscopic phase separation of the solvent, triggered by the mutual insolubility of the alcohol and a PEG/Ti−oxo complex,[25] leads to a macroporous structure. In the synthesis conditions of this work, the intimate interactions between PEG and the Ti−oxo building blocks lead to the formation of a hybrid organic−inorganic wall. Further incompatibility of the PEG and the Ti−O−Ti networks upon film drying leads to a second phase separation in the mesoscale, which in turn leads to the appearance of mesopores. Both phase separation processes seem to occur independently at different scales, as the mesoporous structure has been found in nonmacroporous systems issuing from PEG-containing films. The processes and interactions leading to this hierarchical pore structure are sketched in Scheme 1.

(4) Film Functionalization. The presence of mesopores in these films is interesting because of the possibility of incorporating organic functions in the pore system, leading to surface-modified multiscale porous films.[22,38] Adsorption and grafting experiments were performed to determine the accessibility of the whole pore system. Molecules presenting phosphate or bisphenol grafting groups and a given organic function were used, as reported in previous work with mesoporous titania thin films.[38] The pending organic functions can present different features such as hydrophobicity, hydrophilicity, heavy metal adsorption, and ability to form metal complexes.

Functionalization was carried out in macro-mesoporous films (M) and transparent mesoporous films (T). Uptake experiments were also performed on dense films (D) as a control experiment. Molecule incorporation into the films was followed by two spectroscopic techniques: (1) FTIR of DHDP uptake in films D, T, and M, immersed into a 0.01 M DHDP solution in tetrahydrofurane (THF) and (2) UV−vis spectra of TIRON uptake in transparent films (D and T) immersed in an aqueous 0.01 M solution of TIRON.

Figure 7a shows a comparison of the TIRON uptake on T and D films. An important increase in the signal derived from TIRON adsorption is observed in mesoporous films (T) compared to the D films, similar to those obtained in ordered mesoporous versus dense titania films.[38] Analogous results

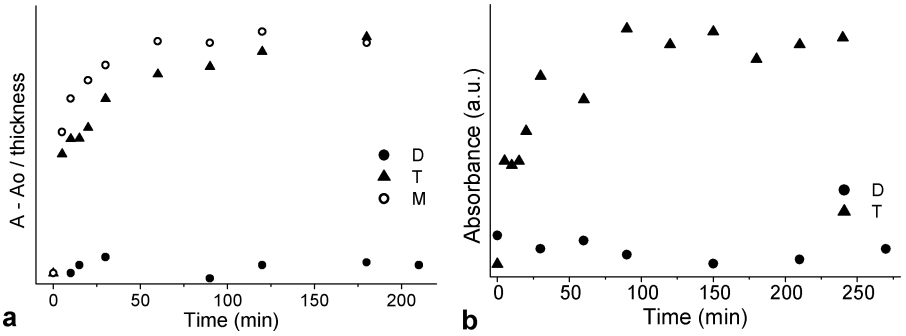

Figure 7. (a) DHDP uptake in M, T, and D films. (b) TIRON uptake in T and D films.

were obtained for the DHDP uptake as a function of time for films D, T, and M. The increase of the ν_{CH} band area of DHDP relative to the film thickness $(A - A_0)/e$ is presented in Figure 7b. Two interesting additional features can be observed:

(a) No substantial differences in molecule adsorption between both porous films are observed. It can be concluded that the accessible area is generated mostly by the mesopores observed in the previous section and that the macropore contribution to the total area is not significant.

(b) The molecule incorporation rate in the M films is slightly higher than in the T films. This suggests that the presence of macropores improves molecule transport in the macro-mesoporous systems compared to the pure mesoporous ones.

(5) Nanocrystalline Macroporous Films. For many TiO_2 technological applications (catalysis, photocatalysis, photovoltaics, etc.), it is important to obtain nanocrystalline films. With the usual thermal treatment done to consolidate TiO_2 structure and eliminate PEG (2 h at 250 °C), the obtained TiO_2 films are amorphous. Films supported on glass substrates suffer stress during crystallization, and this process generates cracks. Thus, postprocessing and thermal treatment must be thoroughly controlled to obtain crystalline walls without microcracks.

From the literature on mesoporous thin films, it is well-known that an adequate post-synthesis treatment can lead to significant differences in the stability and quality of the final nanocrystalline material.[37,46] Different thermal treatments were performed on the macro-mesoporous films discussed above, by submitting samples to different time intervals at temperatures ranging from 250 °C to 500 °C. Some samples were directly submitted to a temperature treatment, and others were thermally treated after a stabilization process (1 day of aging at 50% RH, followed by 1 day at 60 °C and 1 day at 130 °C before the final thermal treatment). The obtained films were studied by SEM to determine the presence of cracks and by TEM and XRD to evaluate the crystallinity. Figure 8 shows noticeable differences in the pore shape and size distribution of samples submitted directly to 250 or 500 °C or to 250 °C after a stabilization process. It is clear that the stabilization process influences the regularity of the pore

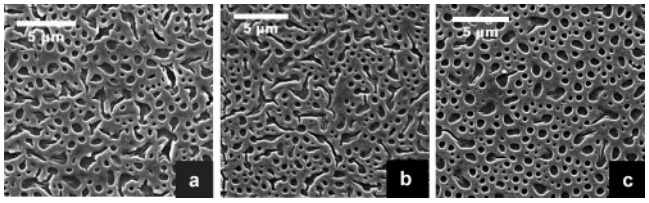

Figure 8. SEM micrograph of films with different thermal treatments: (a) 10 min at 500 °C; (b) 2 h at 250 °C; and (c) previous stabilization + 2 h at 250 °C.

array and helps to strengthen the wall structure, probably by permitting rearrangements in the as-deposited film, while keeping them at controlled high humidity and intermediate temperatures ($T < 150$ °C).[43] In these conditions, film fluidity is ensured by the water contents in the aging atmosphere;[36] at the same time, the high acidity of the initial solutions (protons are likely trapped in the Ti−oxo/PEG deposited gel) relieves the mechanical stress by a gradual condensation process.[7]

In general, films produced with no stabilization process after deposition frequently developed irregular pore systems, and all of them developed cracks after prolonged treatments at $T > 350$ °C. On the other hand, films thermally treated after the stabilization process described above were crack-free and developed well-defined macropores perpendicular to the surface, withstanding treatments at 500 °C for several hours without losing the macroporosity (Figure 9a). No crystal structure was detected by XRD or SAED for the titania samples calcined at $T < 450$ °C. The crystallite sizes for samples calcined at 500 °C, estimated by means of the Scherrer equation (Cu Kα radiation, $\lambda = 1.5418$ Å, and $\beta = 0.03°$, highly crystalline quartz) are presented in Table 2.

TEM-SAED micrographs of high-temperature treated samples show highly crystalline walls made up of anatase. Thermal processing at $T > 500$ °C leads to loss of the mesoporous structure. However, the macroporous texture is not damaged if a suitable post-treatment is made before the calcination (Figure 9a). These nanocrystalline macroporous films can present interesting applications in the photodegradation of species of large size, like bacteria, which are compatible with macropore size.

Conclusions

Titania-based thin films presenting a hierarchical texture with mesoporous walls (2 nm diameter) and macropores (variable between 100 nm and 2 μm diameter) have been synthesized by a combination of sol−gel and phase separa-

(46) (a) Crepaldi, E. L.; Soler-Illia, G. J. A. A.; Grosso, D.; Sanchez, C. *New J. Chem.* **2003**, *1*, 9. (b) Grosso, D.; Soler-Illia, G. J. A. A.; Crepaldi, E. L.; Cagnol, F.; Sinturel, C.; Bourgeois, A.; Brunet-Bruneau, A.; Amenitsch, H.; Albouy, P.-A.; Sanchez, C. *Chem. Mater.* **2003**, *15*, 4562.

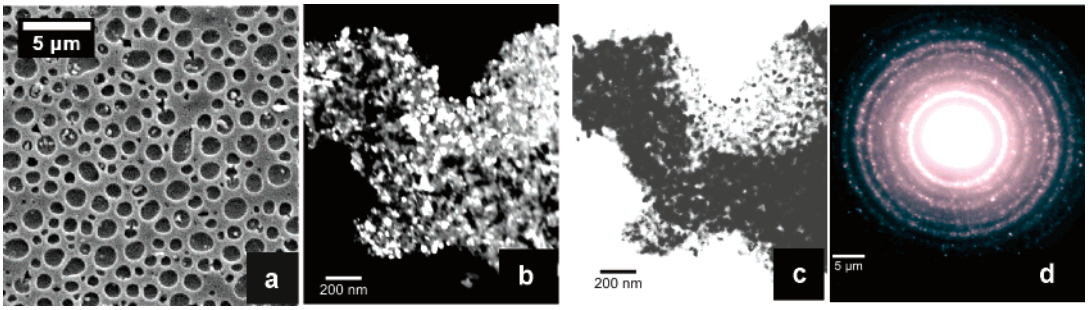

Figure 9. Film calcined for 3 h at 500 °C after a stabilization process: (a) SEM micrograph; (b) TEM dark field image; (c) TEM bright field image; and (d) TEM-SAED image (anatase).

Table 2. Crystallite Sizes Obtained for Samples with Different Thermal Treatments

	thermal treatment				
	3 h at 400 °C	10 min at 500 °C	1 h at 500 °C	2 h at 500 °C	3 h at 500 °C
crystallite size (nm)		5	6	10	27

tion. Processing windows where transparent mesoporous, macro-mesoporous, and cracked textures can be obtained have been found.

While the general procedure of macroporous titania thin film synthesis has been previously reported, this work has disclosed novel structural features. First, in the synthesis conditions reported, nested accessible mesopores are present. This mesostructure is derived from the interactions between the Ti−oxo building blocks and the ethylene oxide blocks in the polymer at the time of film drying and processing. These interactions are coherent with those found in mesoporous titania thin films or xerogels, establishing a bridge between the phenomena taking place in thin textured films formation, whether macro- or mesoporous. Cluster/polymer/solvent interactions and the relative rates of the solidification (by sol−gel processes or drying) and the evaporation processes seem to dominate the phase separation phenomena at the mesoscale; this reinforces the current ideas of macropore formation. The mesopore surface can be modified by post-grafting of organic molecules, leading to a thin film presenting a hierarchical arrangement of porosity scales, one of which can be functionalized. The presence of both types of pores can provide advantages for rapid response functional devices.

An adequate processing of these thin films is essential to obtain regular macropores and, eventually, crack-free macroporous thin films with anatase walls. The role of low-temperature/high-humidity processing in the optimization of the texture and properties has been demonstrated. By adjusting the solution and processing variables, a variety of thin films with different features, from macro-mesoporous functional amorphous titania to highly stable macroporous anatase with variable crystallite size, can be obtained.

Acknowledgment. The authors are deeply indebted to M. Rosenbusch (UAQ-CNEA) for the SEM-EDS characterization, to P. B. Bozzano for the TEM micrographs, and to P. C. Angelomé for help with the functionalization experiments. This work was funded by CONICET (PIP 5191), CNEA, ANPCyT (Grants PICT 06-12057, PICT 06-12345), Fundación Antorchas (14056-18), and Gabbos (RG #17-P&G). Instituto de Tecnología Jorge Sabato, UNSAM, is acknowledged for a grant to M.C.F.; G.J.A.A.S.-I. is a member of CONICET.

CM0527064